Tellus (1990), *42A*, 366–377

Probability density distributions of large-scale midlatitude circulation parameters during Northern Hemisphere summer

By ANDREA BUZZI[1], ANTHONY R. HANSEN[2] and ENNIO TOSI[3], [1]*FISBAT-CNR, Bologna, Italy,* [2]*Meteorology Research Center, Control Data Corporation, Minneapolis, MN, USA,* [3]*Department of Physics, University of Bologna, Bologna, Italy*

(Manuscript received 6 December 1988; in final form 10 April 1989)

ABSTRACT

Probability density estimations of the amplitude of the planetary-scale waves represented by zonal wavenumbers 2–4, the amplitude of the cyclone-scale waves represented by wavenumbers 6–8, and the speed of the zonal mean wind are computed for the middle and high latitudes of the Northern Hemisphere during summer. A 22-year combined NMC and ECMWF dataset is used. The cyclone waves and the zonal mean wind speed exhibit unimodal, nearly normal distributions, whereas the planetary-scale waves exhibit statistically significant bimodality that is not associated with any periodicity in the time series. The differences in physical space between the two statistical flow regimes corresponding to the wave amplitude modes are centered on 60°–65° N. The pattern in the difference field has an equivalent barotropic vertical structure and corresponds in wavelength to wavenumber 3. There is virtually no difference in the structure of the zonal mean flow for the two wave amplitude regimes. The possibility that a resonance may play a role in the summer bimodality is not excluded by the present results.

1. Introduction

The past decade has seen considerable interest in the idea of multiple equilibria or multiple flow regimes in the large-scale atmospheric circulation (e.g., Charney and DeVore, 1979; Wiin-Nielsen, 1979; Hart, 1979; Trevisan and Buzzi, 1980; Reinhold and Pierrehumbert, 1982; etc.). Theoretical investigations have received renewed stimulation recently from observational evidence for the existence of bimodality in the probability density distribution of planetary-scale wave amplitude in Northern Hemisphere (NH) winter (Sutera, 1986; Hansen, 1986; Hansen and Sutera, 1986; Benzi and Speranza, 1987; Molteni et al., 1988). Multiple modes are predicted by theories which include multiple equilibria or more complicated attractors (e.g., Benzi et al., 1984). Although the bimodality in the wave amplitude distribution is a necessary condition for the existence of multiple equilibria, it is not a sufficient condition.

In contrast to the observed wave-amplitude results, the probability density distributions of the speed and shear of the zonally averaged flow during NH winter are unimodal (Sutera, 1986; Hansen and Sutera, 1987). The absence of bimodality in the statistical distribution of the zonal wind speed is a direct contradiction of the result predicted by the original multiple equilibrium theory of Charney and DeVore (1979). However, it has been shown that, by introducing wave–wave nonlinearity, the theory can be reconciled with the observed statistical distributions (Benzi et al., 1986a, b). Most of the existing multiple equilibrium theories generally require that some role be played by the earth's topography, usually in the form of a topographic form-drag instability (e.g., Charney and DeVore, 1979; Charney and Straus, 1980; Reinhold and Pierrehumbert, 1982; Buzzi et al., 1984; Rambaldi and Mo, 1984). However, recent preliminary observational results indicate that planetary wave amplitude bimodality may also be present in the Southern Hemisphere (Hansen and Sutera, 1988), where large-scale, midlatitude topographic forcing does not exist. If this result proves to be statistically significant, it suggests that topographic instabilities may not be relevant to the bimodality.

Previous studies in the NH have focused on winter. In the present paper, we explore the statistical properties of large-scale flow parameters during NH summer to determine the influence of the NH seasonal cycle on the bimodality. The original motivation of this paper was that of extending the statistics of flow parameters, including probability density estimates, to all the seasons other than winter. Here, we discuss briefly some observational characteristics of the annual cycle of flow parameters and explain why we have restricted the presentation to summer results.

The monthly means and standard deviations of planetary wave amplitude (wavenumbers 2–4 indicator: see below for the definition of the indicators) averaged from 45°–75° N, of zonal wind speed (also averaged from 45°–75° N) and of cyclone-scale wave amplitude (wavenumber 6–8 indicator, averaged 30°–60° N) exhibit pronounced seasonal cycles, as shown in Fig. 1. These results are based on 22 years of combined National Meteorological Center (NMC) and European Centre for Medium-Range Weather Forecasts (ECMWF) data. Planetary wave amplitude and standard deviation (the latter computed as the variability within all the same months for the 22 years considered) both present strong annual cycles that are in phase with each other, with no evident harmonics (Fig. 1a). Both quantities change by about a factor of two between winter and summer. The zonal mean wind and its standard deviation in mid-high latitudes behave differently in that wind speed exhibits clear annual and higher harmonic cycles, while its standard deviation has a predominantly annual cycle (Fig. 1b). The maximum wind variability occurs in mid to late winter while the maximum wind speed is present in mid to late fall. The seasonal cycles of cyclone-wave activity and of its standard deviation resemble the zonal wind mean speed, having both annual and higher harmonics, with the largest values attained in spring and late fall (Fig. 1c). This is consistent with Oerlemans (1980) findings that the largest synoptic scale eddy fluxes (a proxy for baroclinic activity) occur in fall and spring in the Northern Hemisphere.

All the above observational results indicate, as noted, for example, by Oerlemans (1980) and Fleming et al. (1987), that discussing the general circulation in terms of winter-mean and summer-mean only, while assuming that behavior in the transition seasons is simply a linear combination of winter and summer behavior, is misleading. However, obtaining meaningful probability estimates of the above flow indicators in the spring and fall seasons is problematic because the strong intra-seasonal trend in the variance renders the time-series non-stationary within these seasons. Therefore, we restrict our analysis to the summer period only (JJA), when all the indicators considered in Fig. 1 exhibit absolute minima.

Further observational results and discussion of dynamical aspects of NH summer climatology can be found in the classical literature (e.g., Palmén and Newton, 1969). White (1982) and Wallace (1983) describe the difference of stationary planetary wave structure between summer and winter. White (1982) also discusses the possible relative importance of topographic and thermal forcing of midlatitude stationary waves and the characteristics of transient eddies. In mid to high latitudes, the NH summer contrasts with winter essentially in that a reversal of the stationary midlatitude thermal forcing takes place and the zonal wind changes substantially. The NH summer climatology represents a very different realization of the atmospheric circulation from the winter climatology.

2. Data and procedures

The primary data used in this study consists of daily 500 mb height analyses on a 5° by 5° latitude–longitude grid for the 22 years from 1 January 1964 through 31 December 1985. These analyses were compiled by NMC from 1 January 1964 to 31 December 1980 and by ECMWF from 1 January 1980 to 31 December 1985. Time series of variables of interest were constructed after

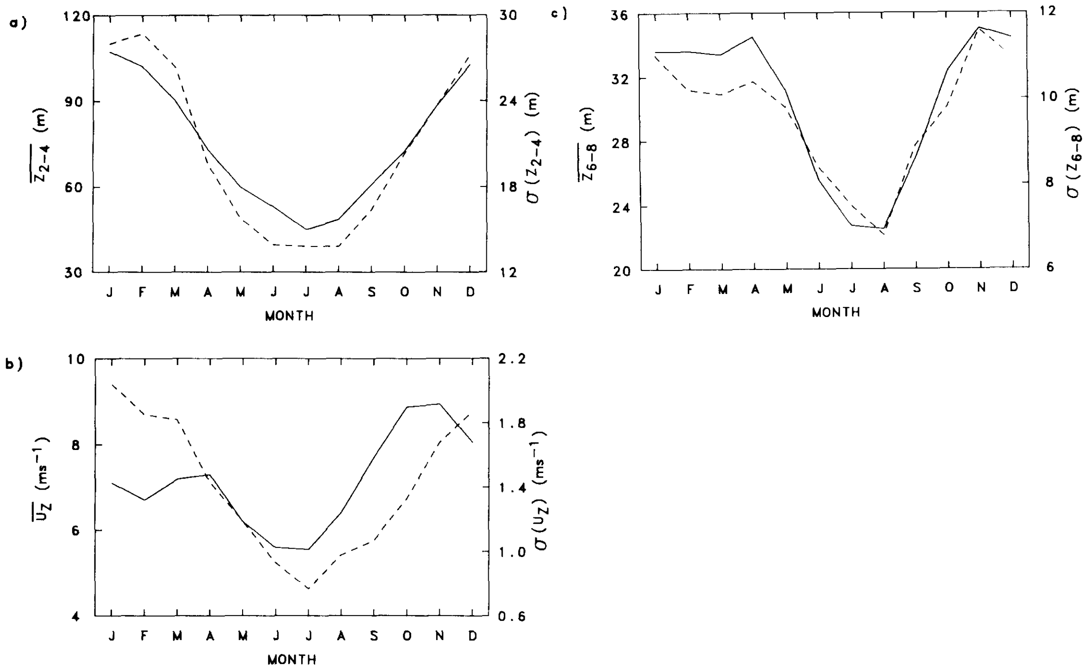

Fig. 1. Annual march of the monthly means (solid lines) and daily standard deviation from the monthly means (dashed lines) at 500 mb based on 22 years of combined NMC and ECMWF data for (a) the amplitude of waves 2 through 4, Z_{2-4}, (b) the zonal wind speed, U_z and (c) the amplitude of waves 6 through 8, Z_{6-8}. These values are obtained after averaging the data between 45° and 70°N in (a) and (b) and between 30° and 60°N in (c).

joining the two sets of analyses at 1 June 1980. Intercomparisons made using the overlapping period of the two analyses indicated marginal differences between them for the present purposes. As expected, departures between the two analyses are more appreciable for higher zonal harmonics. For example, wavenumbers 6–8 in the ECMWF analyses have roughly 5% larger amplitudes, on average, compared to NMC analyses.

We examine 2 different wave groups: the planetary waves represented by zonal wavenumbers 2 to 4 and the cyclone-scale wavenumbers represented by wavenumbers 6 to 8. The former wavenumber group corresponds to that studied earlier for winter (Sutera, 1986; Hansen and Sutera, 1986). Waves 6 to 8 represent the middle of the major baroclinic energy producing region of the transient eddy spectrum (e.g., Saltzman, 1970) and are taken as representative of the transient, cyclone-scale eddies. For each of the 8036 days in the dataset, the root mean square values of the wave amplitudes were computed after zonal harmonic analysis of the latitudinally averaged 500 mb heights from

$$[Z_{2\text{-}4}] = \left(\sum_{m=2}^{4} 2 Z_m \cdot Z_m^* \right)^{1/2}$$

and

$$[Z_{6\text{-}8}] = \left(\sum_{m=6}^{8} 2 Z_m \cdot Z_m^* \right)^{1/2}$$

where Z_m in either case is the complex coefficient for wavenumber m of the grid point heights averaged arithmetically between latitudes ϕ_1 and ϕ_2 (Z_m^* denotes the complex conjugate of Z_m). The planetary waves are analyzed in the latitude zone from 45°N to 70°N. This is the same zone as chosen by Hansen and Sutera to reduce the impact of interannual variability and to optimize the information content attainable from the

NMC gridded analyses. This zone was retained because one goal of the analysis is examination of the statistical properties of the planetary waves in a westerly flow. In summer, the latitude of maximum wave 2–4 activity at 500 mb shifts to 65° N from 55° N in winter (see also White, 1982) and the maximum zonal mean westerlies occur at 45° N. The region of maximum wave activity is contained within the zone of the analysis throughout the year. The cyclone-scale wave amplitude is computed in the latitude zone from 30°–60° N because the cyclone waves maximum mean values remain in this zone throughout the year, ranging from peak values at 45° N in winter to 50° N in summer.

The average geostrophic zonal wind speed in the 45° N to 70° N zone is computed on each day following Hansen and Sutera (1987) from

$$[U_Z] = \frac{1}{\sin\phi_2 - \sin\phi_1} \int_{\phi_1}^{\phi_2} \frac{-g}{f} \frac{1}{a} \frac{\partial \bar{z}(\phi)}{\partial \phi} \cos\phi \, d\phi,$$

where $\bar{z}(\phi)$ is the zonal mean 500 mb height at latitude ϕ. The factor to the left of the integral sign results from an area averaging of the zonal wind speed.

Prior to making the probability density estimations, the resulting time series of these variables were filtered by means of FFT decomposition of the time series and resynthesis after removing unwanted frequencies as was done in the earlier studies. Each of the three time series was filtered to remove the annual period and its harmonics and high frequency variability that could be associated with noise in the time series. The $[Z_{2\text{–}4}]$ time series was filtered to remove the annual cycle (no evident harmonics of the annual cycle were present, see Fig. 1a) and high frequency variance with periods less than 4 days. The zonal wind speed was treated similarly with the annual cycle and its harmonics and periods shorter than 4 days removed. Sensitivity of the results to details of the filtering are discussed in the following sections. The cyclone-scale waves represented by $[Z_{6\text{–}8}]$ were treated slightly differently. In particular, power spectral analyses reveal that wavenumbers 6–8 in summer are dominated by eastward traveling waves with periods of 4 to 15 days. An additional problem is the strong seasonal trend in the variance during summer illustrated in Fig. 1c. Therefore, the 22 year time series of this cyclone-scale wave amplitude was filtered to remove fluctuations at the high frequency end of the spectrum that are poorly resolved by our daily data (filter tapered from response of 1 at 3 days to response of 0 at 2 days) and periods much longer than those associated with traveling cyclones (all periods > 90 days).

After filtering each time series, composite summer data samples were formed by extracting the June, July and August data for each year. Each summer data composite then consists of 2024 observations. Of these, based on the autocorrelation functions, roughly 440 of the $[Z_{2\text{–}4}]$ values may be considered independent. The $[Z_{6\text{–}8}]$ time series contains approximately 800 independent samples and the $[U_Z]$ time series at most 200.

Since the probability density distributions are not known, they are estimated using the nonparametric maximum penalized likelihood (MPL) method. The merits of this technique have been discussed by Hansen and Sutera (1986, 1988). The MPL technique includes a tunable parameter often called the "smoothness" parameter, denoted here as α. The challenge of using the MPL technique is in choosing α to yield statistically significant results. The numerical value of α leading to significant results is a function of the number of independent samples in the dataset and also of the variance or range of the data sample. Statistical simulation techniques (Silverman, 1981; Hansen and Sutera, 1986) are used to establish whether a given multimodal estimate may be obtained by random chance from any given parent distribution. As will be shown, for the present data the simplest unimodal parent distribution is a normal distribution having the same mean and standard deviation as the data. Therefore, ensembles of random numbers were drawn from a normal parent distribution and were analyzed using the MPL technique (after truncation of outlier points as done with the data, see Subsection 3.1) for a range of α values to establish the probability that multiple modes obtained for a given value of α could occur by random chance. Statistical significance is determined by comparing the (normalized) value of α for which any bimodality might be obtained to the results of the statistical simulations. The number of mesh points used in the individual estimates was chosen to give roughly

2 m between mesh points for the wave amplitude estimates and 0.10 m s^{-1} for the zonal wind speed estimates.

3. Results

3.1. Probability density estimates

The results of the probability density estimations for the planetary and cycle-scale wave amplitude, and zonal wind speed are presented in Fig. 2. In each case, estimates for two values of α are given. These values correspond to 99% and 95% confidence in the statistical significance of any multiple modes compared to the null hypothesis that the data are normally distributed. For each data sample, outlier points were truncated from the tails of the distribution (4% of the total sample or 80 observations truncated from each tail) prior to the MPL estimate.

The results indicate that the planetary wave group exhibits bimodality while the cyclone-scale waves and zonal wind speed are unimodal. In fact, the distributions for the zonal wind speed and cyclone-scale wave amplitude depart very little from normal distributions. The notch near the low amplitude tail of the $[Z_{6-8}]$ estimate (Fig. 2c) becomes a mode as α is further reduced, but its presence is unstable to minor changes in tail truncation or filtering. In summer, the two modes of the planetary-scale distribution in Fig. 2a are separated by ~ 12 m which is about one standard

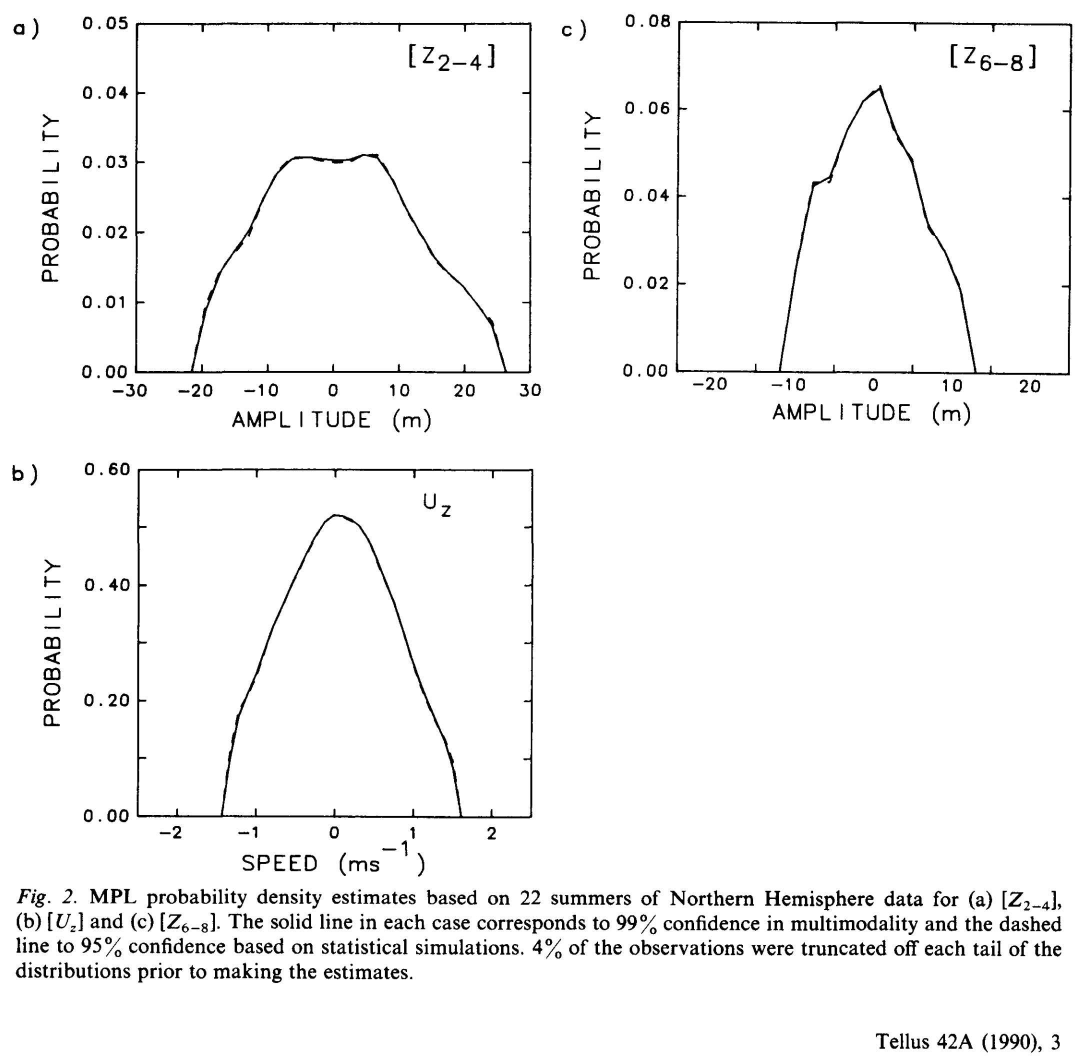

Fig. 2. MPL probability density estimates based on 22 summers of Northern Hemisphere data for (a) $[Z_{2-4}]$, (b) $[U_z]$ and (c) $[Z_{6-8}]$. The solid line in each case corresponds to 99% confidence in multimodality and the dashed line to 95% confidence based on statistical simulations. 4% of the observations were truncated off each tail of the distributions prior to making the estimates.

deviation of the distribution. This value can be compared with the ~21 m separation in winter (Hansen and Sutera, 1986) which is also close to the winter standard deviation. The minimum in the 22 summer planetary wave amplitude distribution is relatively shallow compared to that in winter which is partially the result of strong interannual variability which could not be filtered. Note also that almost equal probability pertains to the 2 modes in summer (unlike winter).

The shallowness of the planetary wave distribution's minimum is largely due to the NMC data sample. If the analysis is repeated using the NMC summers and ECMWF summers separately, the individual composites are also bimodal, but the minimum is much deeper and appears at much larger and therefore more statistically significant α values in the 6 summers of ECMWF data than in the 16 summers of NMC data (not shown). In view of this, an a posteriori reconsideration of the NMC data is given at the end of Subsection 3.2.

Some sensitivity in the details of the shape of the $[Z_{2-4}]$ distribution was noted due to the cutoff frequency and tapering of the high frequency filter. The bimodality is robust to changes in the filter, but the position of the modes and the minimum may shift slightly, and the statistical confidence in the bimodality may be reduced (from 99% in Fig. 2a to 95% or lower) due, for example, to changing the high frequency cut off or by tapering the high frequency end of the filter more or less. Again, the NMC data taken alone were more sensitive in this regard than the ECMWF data. In addition, the summer data are more sensitive in this regard than the winter data.

Bimodal probability density estimations would, of course, result from periodic time series. As discussed previously (Hansen and Sutera, 1986), if a periodicity were responsible for the bimodality, a peak should appear in the probability density of duration of events in each mode but none was found (not shown).

3.2. *Physical space structure*

It is of interest to examine the mean physical space structure of the atmosphere associated with the summer bimodality in order to build confidence in the physical significance of the result. Geopotential height analyses at 850, 500, and 300 mb from NMC for the years 1964–80 were available for this part of the study. These analyses were partitioned according to the value of the planetary wave amplitude indicator on each summer day. Grids for which the 500 mb planetary wave amplitude was less than the minimum in Fig. 2a were consigned to the mode 1 composite for each level. Grids for which the amplitude was greater than the minimum were included in the mode 2 composite for each level. The composite mode 1 and mode 2 eddy fields (i.e., departure from zonal symmetry) as well as the difference between them is presented in Figs. 3–5.

The difference between the two summer modes is primarily a high-latitude pattern centered on 60°–65° N (Fig. 5). Four major features appear in the difference field: lows centered over the North Pacific and near Baffin Island, and highs over northwestern Canada and Scandinavia. Note that the amplitude of the pattern in the difference field is comparable to the amplitude of the mode 1 mean eddy field at high latitudes. The vertical structure of the difference field is equivalent barotropic and the amplitude grows with height. The dominant wavelength of the pattern in the difference field corresponds to zonal wavenumber 3. The most evident differences are confined to the north side of the maximum in the zonal mean westerlies which is at 45° N during summer. Lower latitude baroclinic features such as the monsoon low over southern Asia at lower levels and the subtropical highs over the Atlantic and eastern Pacific are virtually identical in the composite mode 1 and mode 2 eddy fields (Figs. 3, 4). In addition, the average latitudinal profiles of the zonal mean geostrophic wind averaged for each planetary wave mode at 850, 500, and 300 mb are very similar to one another (not shown), and the vertical shear of the zonal flow is virtually identical for the two modes.

It is interesting, at this point, to compare the summer mode 2 − mode 1 difference pattern with the corresponding winter pattern. We cannot expect, a priori, a strong resemblance between the two, considering that stationary eddy climatology differs substantially between the two seasons (Wallace, 1983). Nevertheless, we can see, by comparing Fig. 5 here with Fig. 15 of Hansen and Sutera (1986), that the summer mode

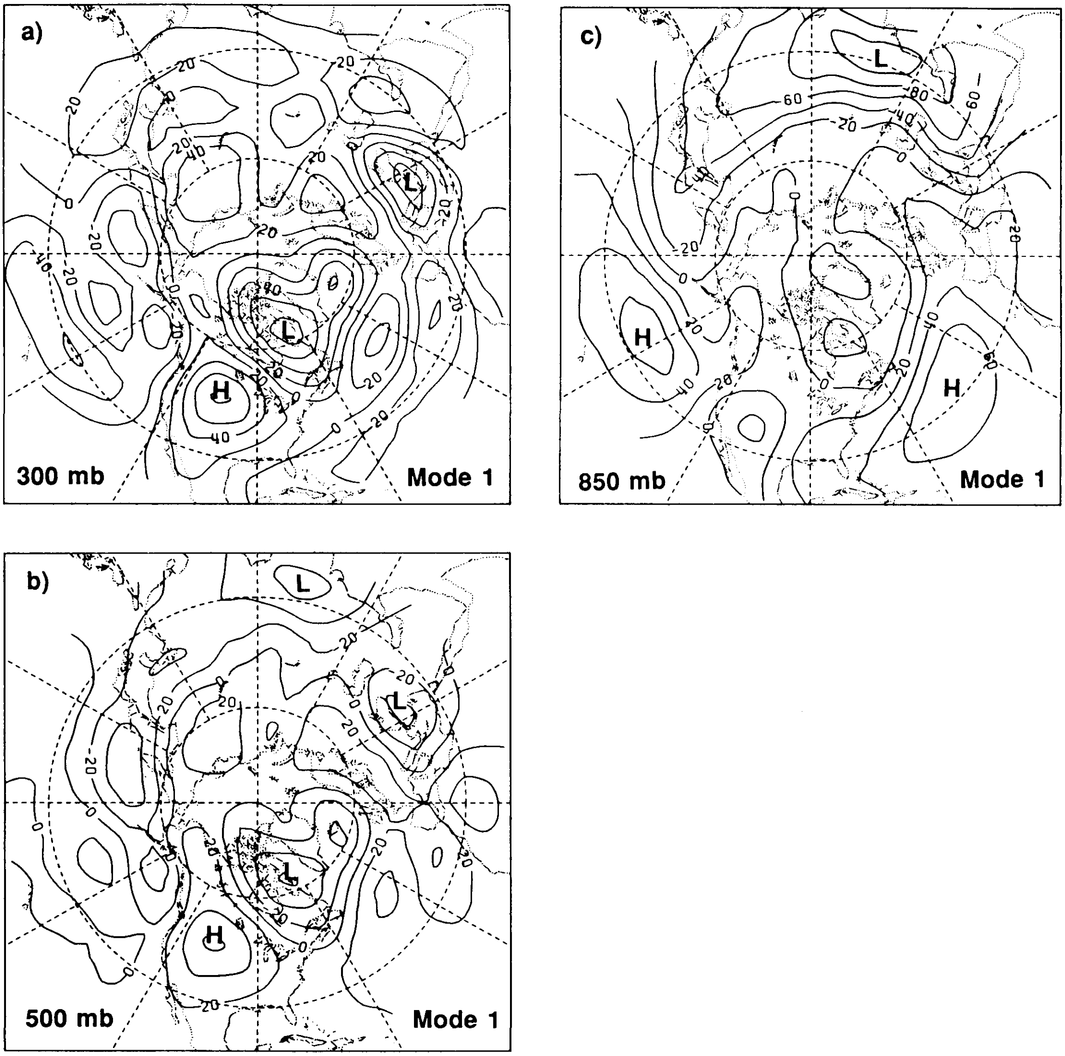

Fig. 3. Mean geopotential height maps for the eddy field composited from all mode 1 days (1964–80) at (a) 300 mb, (b) 500 mb, and (c) 850 mb. The contour interval is 20 m.

2 − mode 1 difference is reminiscent of the winter difference more than are the stationary waves, although the amplitude is about a factor of 2 smaller and some features are slightly smaller in scale in summer than in winter. In particular, we note an eastward shift, from winter to summer, of the negative–positive couplet over the Pacific and north-west American sector (this reflects a similar shift that occurs in the stationary eddy field over the same region), but further to the east the negative center over the Baffin Island and the positive center just to the west of Scandinavia are nearly in the same locations in the two seasons. It is interesting to note the fairly close correspondence of the locations of positive difference centers in Fig. 5 with the locations of most frequent blocking during summer (e.g., Lejenäs and Økland, 1983).

One of the possible explanations of the bimodality is a mechanism involving topographic

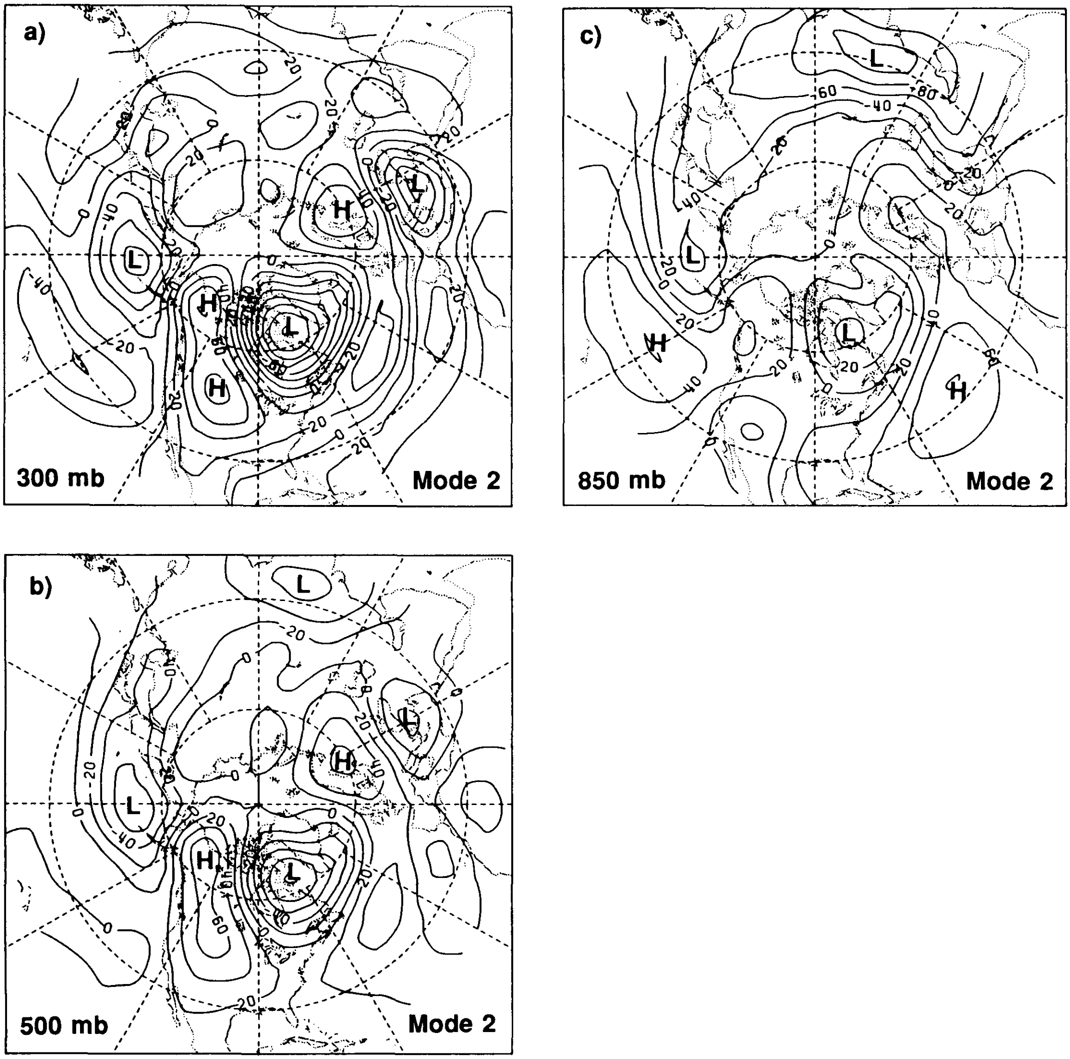

Fig. 4. Mean geopotential height maps for the eddy field composited from all mode 2 days (1964–80) at (a) 300 mb, (b) 500 mb, and (c) 850 mb. The contour interval is 20 m.

resonance. Although it is far from clear whether resonance has any relevance to the bimodality (Hansen and Sutera, 1988) it is nonetheless interesting to explore the possibility. Simple linear ray tracing ideas have been used, among other things, to investigate whether resonant waves might be trapped in midlatitudes due to the structure of the zonal flow (e.g., Hoskins and Karoly, 1981; Held, 1983). Following Held (1983), the stationary zonal wavenumber satisfying a steady, linear vorticity equation with a sinusoidal wave solution for the streamfunction is

$$n_s = aK_s = \left(\cos\phi\left(\beta + \frac{1}{a}\frac{\partial \zeta_z}{\partial \phi}\right)\right) \Big/ (U_z/\cos\phi),$$

where a is the earth's radius, ϕ latitude, subscript z denotes zonal averaging, ζ is the relative vorticity and other notation is conventional. The determination of n_s for both mode 1 and mode 2

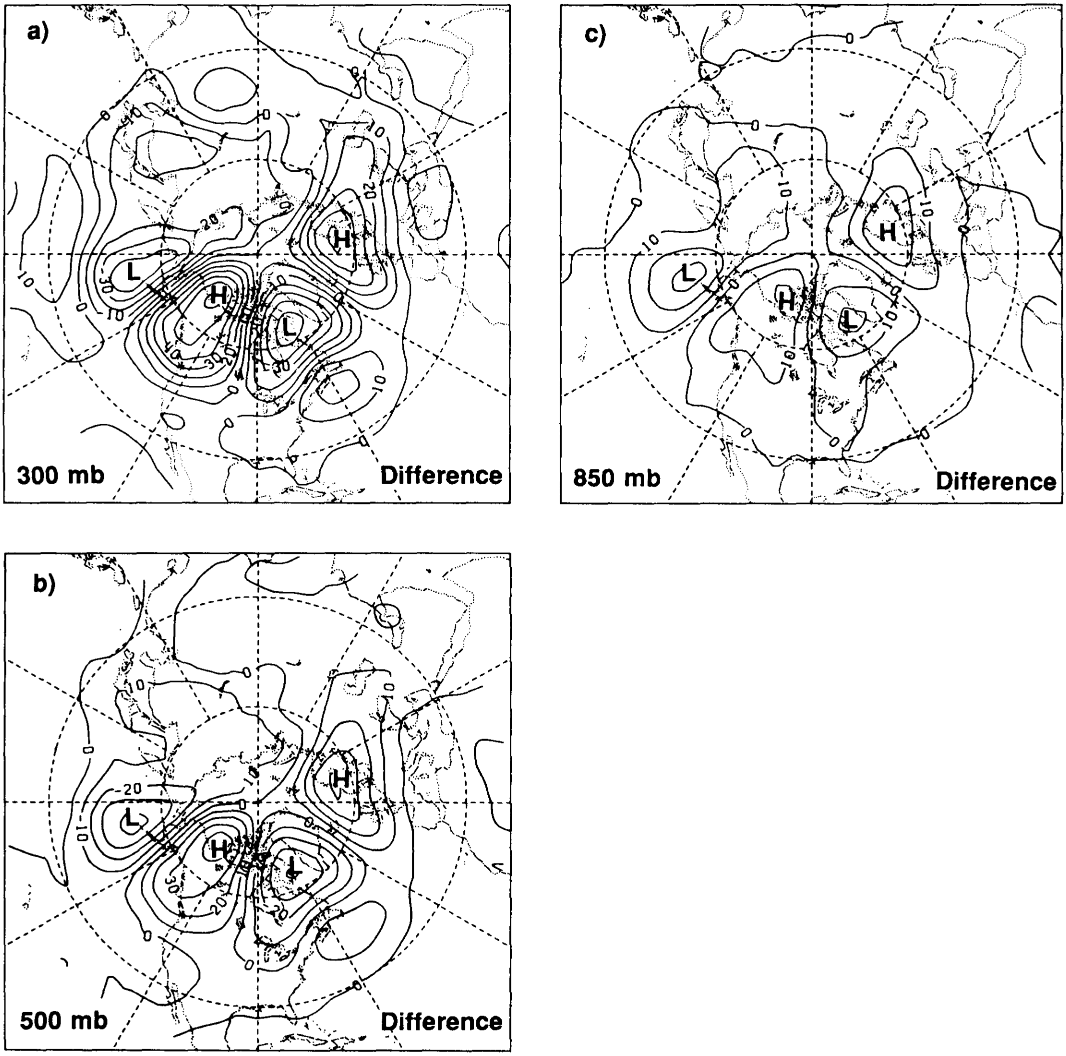

Fig. 5. The difference between mean mode 2 eddy field and the mean mode 1 eddy field in Figs. 3 and 4 at (a) 300 mb, (b) 500 mb, and (c) 850 mb. The contour interval is 10 m.

mean conditions at 300 mb in summer is presented in Fig. 6. As can be seen, the possibility of trapping wavenumber 3 and higher exists north of 45° N. Since n_s can be thought of as an index of refraction, waves would be refracted towards the largest n_s (Held, 1983). Thus, the largest amplitudes might be expected at 60° N where n_s is the largest. This is near the latitude of the largest eddy differences between the modes. Cautious interpretation of this result is necessary, however, because the zonal flow undergoes substantial fluctuations so the steady state assumptions involved in the derivation of n_s may not be valid.

The maps in Fig. 5 indicate a substantial difference between the mean height fields corresponding to the two modes in roughly the 55°–75° N zone with a predominant wavelength very close to that of wavenumber 3 as noted above. The fact that this difference appears between the mean heights of the two modes is

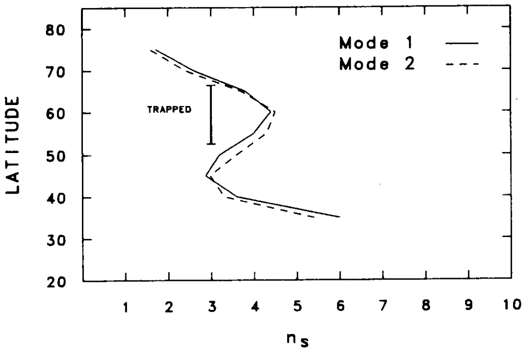

Fig. 6. Stationary zonal wavenumber n_s for each mode's composite 300 mb geostrophic wind profile. The potential for midlatitude confinement of zonal wavenumber 3 and higher north of 45° N is indicated.

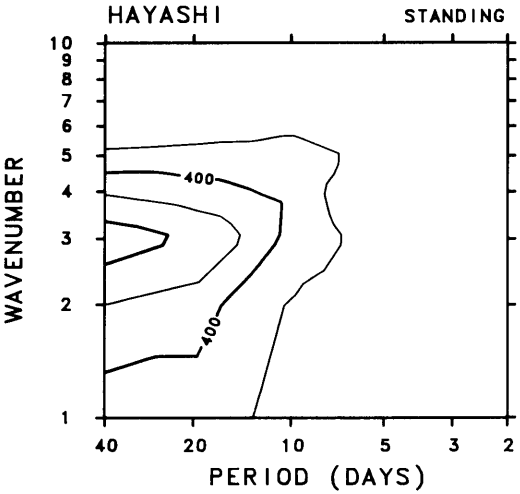

Fig. 7. Power spectral density of the standing variance for the NH summer 500 mb geopotential height averaged between 55° N and 75° N determined by the Hayashi (1979) technique. The contour interval is 200 m^2. The power was normalized by the wavenumber and frequency for the log–log presentation. The results are computed from 120-day data segments (mid-May to mid-September) from each summer using a Tukey window and 20 day lags.

indicative of the presence of a standing oscillation in the NH summer. The presence of this standing variance can be confirmed by computing the power spectrum of the standing variance (Hayashi, 1979) at 500 mb for geopotential height averaged between 55° N and 75° N (Fig. 7). (See

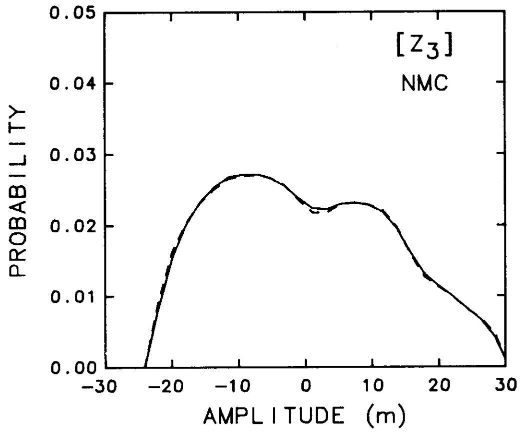

Fig. 8. Probability density estimate of the amplitude of wavenumber 3 based on 17 summers (1964–80) of NMC data for the 55°–75° N zone. The results for 2 values of α are presented which correspond to 99% (solid line) and 95% (dashed line) statistical significance.

Hansen et al., 1989, and references therein for further discussion of the interpretation of power spectra results.) The strongest power in the standing variance spectrum appears at wavenumber 3 (for periods longer than roughly 15 days) consistent with the difference maps as expected. By repeating the MPL analysis for wavenumber 3 only in the 55°–75° N zone, the NMC data exhibit a very strong bimodality (Fig. 8). The value of the smoothness parameter α for which the bimodality was obtained exceeds 99% confidence in the statistical significance in this result for this sample.

4. Conclusion

Probability density estimations of the amplitude of the planetary-scale waves (zonal wavenumbers 2–4), cyclone-scale waves (represented by zonal wavenumbers 6–8) and the speed of the zonal mean wind were computed for the middle and high latitudes of the Northern Hemisphere during summer from a 22 year NMC and ECMWF combined dataset. The cyclone-scale waves and the zonal flow exhibit unimodal, nearly normal distributions whereas the planetary waves exhibit statistically significant bimodality.

The two modes in summer are separated by roughly half of the winter value but the standard deviation of the 500 mb planetary waves is similarly reduced during summer compared to winter. The zonal wind speed is reduced in middle and high latitudes by a similar factor in summer compared to winter in the Northern Hemisphere. The differences between the mean circulations corresponding to the two summer modes are centered on 60°–65° N. The dominant wavelength of the pattern in the difference field corresponds to zonal wavenumber 3 and it has an equivalent barotropic vertical structure. The possibility that a mechanism involving resonance may play a role in the summer bimodality is not excluded by the present results.

5. Acknowledgements

We wish to thank Dr. A. Sutera and Dr. A. Speranza for useful and stimulating discussions during the course of this work. This study was supported by the Climate Dynamics Program of the National Science Foundation under grants ATM-8518507 and ATM-8721728 at Control Data, and by research funds of the Italian Ministry of Public Education and of the CNR.

REFERENCES

Benzi, R., Hansen, A. R. and Sutera, A. 1984. On stochastic perturbation of simple blocking models. *Q. J. Roy. Met. Soc. 110*, 393–409.

Benzi, R., Malguzzi, P., Speranza, A. and Sutera, A. 1986a. The statistical properties of general atmospheric circulation: observational evidence and a minimal theory of bimodality. *Q. J. Roy. Met. Soc. 112*, 661–674.

Benzi, R., Speranza, A. and Sutera, A. 1986b. A minimal baroclinic model for the statistical properties of low frequency variability. *J. Atmos. Sci. 43*, 2962–2967.

Benzi, R. and Speranza, A. 1987. Dynamics and statistics of atmospheric low frequency variability. In: *Irreversible phenomena and dynamical systems analysis in geosciences* (eds. C. Nicolis and G. Nicolis). Dordrecht: Reidel Publ. Co., 199–239.

Buzzi, A., Trevisan, A. and Speranza, A. 1984. Instabilities of a baroclinic flow related to topographic forcing. *J. Atmos. Sci. 41*, 637–650.

Charney, J. G. and DeVore, J. G. 1979. Multiple flow equilibria in the atmosphere and blocking. *J. Atmos. Sci. 36*, 1205–1216.

Charney, J. G. and Straus, D. M. 1980. Form-drag instability, multiple equilibria and propagating planetary waves in baroclinic, orographically forced planetary wave systems. *J. Atmos. Sci. 37*, 1157–1176.

Fleming, E. L., Lim, G.-H. and Wallace, J. M. 1987. Differences between the spring and autumn circulation of the Northern Hemisphere. *J. Atmos. Sci. 44*, 1266–1286.

Hansen, A. R. 1986. Observational characteristics of atmospheric planetary waves with bimodal amplitude distributions. *Adv. in Geophys. 29*, 101–133.

Hansen, A. R. and Sutera, A. 1986. On the probability density distribution of planetary-scale atmospheric wave amplitude. *J. Atmos. Sci. 43*, 3250–3265.

Hansen, A. R. and Sutera, A. 1987. The probability density distribution of the speed and horizontal and vertical shear of the zonal-mean flow. *J. Atmos. Sci. 44*, 1525–1533.

Hansen, A. R. and Sutera, A. 1988. Planetary wave amplitude bimodality in the Southern Hemisphere. *J. Atmos. Sci. 45*, 3771–3783.

Hansen, A. R., Sutera, A. and Venne, D. E. 1989. An examination of midlatitude power spectra: evidence for standing variance and the signature of El Niño. *Tellus 41A* (in press).

Hart, J. E. 1979. Barotropic quasi-geostrophic flow over anisotropic mountains. *J. Atmos. Sci. 36*, 1736–1746.

Hayashi, Y. 1979. A generalized method of resolving transient disturbances into standing and traveling waves by space-time spectral analysis. *J. Atmos. Sci. 36*, 1017–1029.

Held, I. M. 1983. Stationary and quasi-stationary eddies in the extra tropical troposphere: theory. In: *Large-scale dynamical processes in the atmosphere* (eds. B. Hoskins and R. Pearce). London and New York: Academic Press, 127–168.

Hoskins, B. J. and Karoly, D. 1981. The steady linear response of a spherical atmosphere to thermal and orographic forcing. *J. Atmos. Sci. 38*, 1179–1196.

Lejenäs, H. and Økland, H. 1983. Characteristics of Northern Hemisphere blocking as determined from a long time series of observational data. *Tellus 35A*, 350–362.

Molteni, F., Sutera, A. and Tronci, N. 1988. EOF's of the geopotential eddies at 500 mb in winter and their probability density distributions. *J. Atmos. Sci. 45*, 3063–3080.

Oerlemans, J. 1980. An observational study of the upward sensible heat flux by synoptic-scale transients. *Tellus 32*, 6–14.

Palmén, E. and Newton, C. W. 1969. *Atmospheric circulation systems: their structure and physical interpretation.* International Geophysics Series 13. New York: Academic Press, 603 pp.

Rambaldi, S. and Mo, K. C. 1984. Forced stationary solutions in a barotropic channel: multiple equilibria and theory of nonlinear resonance. *J. Atmos. Sci. 41*, 3135–3146.

Reinhold, B. B. and Pierrehumbert, R. T. 1982. Dynamics of weather regimes: quasi-stationary waves and blocking. *Mon. Wea. Rev. 110*, 1105–1145.

Saltzman, B. 1970. Large scale atmospheric energetics in the wavenumber domain. *Rev. Geophys. Space Phys. 8*, 289–302.

Silverman, B. W. 1981. Using kernel-density estimators to investigate multimodality. *J. Roy. Stat. Soc. B43*, 97–99.

Sutera, A. 1986. Probability density distribution of large-scale atmospheric flow. *Adv. in Geophys. 29*, 227–249.

Trevisan, A. and Buzzi, A. 1980. Stationary response of barotropic weakly nonlinear Rossby waves to quasi-resonant orographic forcing. *J. Atmos. Sci. 37*, 947–957.

Wallace, J. M. 1983. The climatological mean stationary waves: observational evidence. In: *Large-scale dynamical processes in the atmosphere* (eds. B. Hoskins and R. Pearce). London and New York: Academic Press, 27–53.

White, G. H. 1982. An observational study of the Northern Hemisphere extratropical summertime general circulation. *J. Atmos. Sci. 38*, 28–40.

Wiin-Nielsen, A. 1979. Steady states and stability properties of a low-order, barotropic system with forcing and dissipation. *Tellus 31*, 375–386.